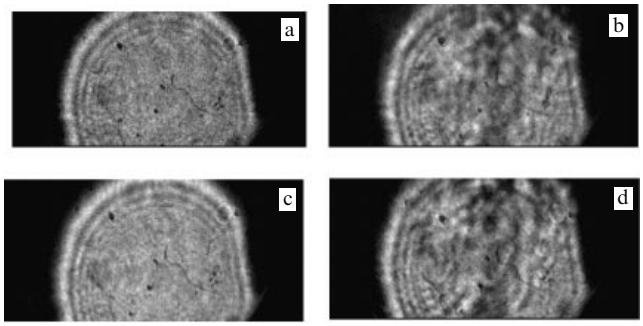

Figure 5. Far-field photoluminescence intensity distribution patterns obtained through windows in a metallic mask. The patterns correspond to the optical Fourier transform of a real spatial luminescence structure ($T = 1.7$ K). The pairs of images in Figs 5a and 5b and in Figs 5c and 5d correspond to two different 5 μm windows in a metallic mask. The patterns in Figs 5a and 5c were obtained for a low pump power, when the spatial intensity distribution in the window is structureless; the patterns in Figs 5b and 5d were obtained for a substantially higher pump power (about 90 μW), when a spatial luminescence structure with the hexagonal symmetry appears in the window, which is similar to the structure shown in Figs 4a – 4d.

tureless. In this case, the far-field intensity distribution is also uniform. We emphasize that the concentric interference fringes observed in the far-field patterns are due to diffraction by the exit pupil of the optical system and bear no direct relation to the subject under discussion. The situation is significantly different in the operation with a higher-intensity pump (about 90 μW in power), when a spatially periodic luminescence structure with the hexagonal symmetry similar to that shown in Figs 4a – 4d is observed in the window. Under these conditions, the far-field patterns depicted in Figs 5b and 5d clearly exhibit the effect of destructive interference (the intensity dip at the center of the far-field pattern), which is qualitatively consistent with the theoretical predictions in Ref. [14]. The above experimental observations are one of the manifestations of the coherence of the collective interwell exciton state in the conditions of Bose condensation in a lateral trap. Furthermore, the discovery of the destructive interference in the far-field patterns is an indication that the luminescence intensity of the condensed exciton phase has a manifest angular directivity relative to the normal to the structure surface, which is a salient feature of superradiance [22].

At the same time, the question of the extent to which the system of interwell excitons is electrically neutral remains open. An attempt to answer this question invites investigations of interwell exciton condensation under the resonance photoexcitation conditions.

Acknowledgements

To conclude, the authors express their gratitude to S V Iordanskii, L V Keldysh, I V Kukushkin, Yu M Kagan, V D Kulakovskii, V G Lysenko, and G M Eliashberg for the numerous discussions, and to S V Dubonos for depositing metallic films of prescribed thickness and electron lithography of the structures. This work was supported by the Russian Foundation for Basic Research.

References

1. Fukuzawa T, Mendez E E, Hong J M *Phys. Rev. Lett.* **64** 3066 (1990)
2. Butov L V et al. *Phys. Rev. Lett.* **86** 5608 (2001)
3. Larionov A V et al. *Pis'ma Zh. Eksp. Teor. Fiz.* **75** 689 (2002) [*JETP Lett.* **75** 570 (2002)]
4. Dremin A A et al. *Pis'ma Zh. Eksp. Teor. Fiz.* **76** 526 (2002) [*JETP Lett.* **76** 450 (2002)]; Gorbunov A V, Bisti V E, Timofeev V B *Zh. Eksp. Teor. Fiz.* **128** 803 (2005) [*JETP* **101** 693 (2005)]
5. Butov L V et al. *Nature* **417** 47 (2002)
6. Butov L V, Gossard A C, Chemla D S *Nature* **418** 751 (2002)
7. Snoke D et al. *Nature* **418** 754 (2002)
8. Rapaport R et al. *Phys. Rev. Lett.* **92** 117405 (2004)
9. Lozovik Yu, Yudson V I *Pis'ma Zh. Eksp. Teor. Fiz.* **22** 556 (1975) [*JETP Lett.* **22** 274 (1975)]; Lozovik Yu E, Berman O L *Zh. Eksp. Teor. Fiz.* **111** 1879 (1997) [*JETP* **84** 1027 (1997)]
10. Ivanov A L, Littlewood P B, Haug H *Phys. Rev. B* **59** 5032 (1999)
11. Zhu X et al. *Phys. Rev. Lett.* **74** 1633 (1995)
12. Snoke D W et al., cond-mat/0410298
13. Gorbunov A V, Timofeev V B *Pis'ma Zh. Eksp. Teor. Fiz.* **80** 210 (2004) [*JETP Lett.* **80** 185 (2004)]
14. Keeling J, Levitov L S, Littlewood P B *Phys. Rev. Lett.* **92** 176402 (2004)
15. Sugakov V I *Solid State Commun.* **134** 63 (2005)
16. Gorbunov A V, Timofeev V B *Pis'ma Zh. Eksp. Teor. Fiz.* **83** 178 (2006) [*JETP Lett.* **83** 146 (2006)]
17. Ketterle W *Rev. Mod. Phys.* **74** 1131 (2002)
18. Chen X M, Quinn J J *Phys. Rev. Lett.* **67** 895 (1991)
19. Keldysh L V *Pis'ma Zh. Eksp. Teor. Fiz.* **23** 100 (1976) [*JETP Lett.* **23** 86 (1976)]; Keldysh L V, Tikhodeev S G *Pis'ma Zh. Eksp. Teor. Fiz.* **21** 582 (1975) [*JETP Lett.* **21** 273 (1975)]
20. Greenstein M, Wolfe J P *Phys. Rev. Lett.* **41** 715 (1978)
21. Kukushkin I V et al. *Phys. Rev. Lett.* **90** 156801 (2003)
22. Dicke R H *Phys. Rev.* **93** 99 (1954)

PACS numbers: 42.62.Be, 42.62.Fi, 42.65.Re
DOI: 10.1070/PU2006v049n06ABEH006044

The unique femtosecond spectrometric complex as an instrument for ultrafast spectroscopy, femtochemistry, and nanooptics

S V Chekalin

1. Introduction. Retrospective excursus

Nearly the last forty years of the fifty-year-long history of quantum electronics have been related to ultrashort laser pulses (USPs) [1]. These light 'bullets' occupy a special place in the history of research in ultrafast process dynamics, because they have facilitated the swiftest progress in the measurement of short time intervals over the last several centuries (Fig. 1). The use of USPs enabled real-time investigations of the dynamics of ultrafast processes that had previously been considered 'experimentally unobservable.' Furthermore, the record-high USP power, which allows realizing light fields that are significantly stronger than intraatomic ones, makes the pursuance of unique experiments feasible [1]. The making of the first USP lasers in the USSR was fostered by the prospect of obtaining record-high powers for the solution of the laser fusion problem. Employing a laser facility [2] developed in the Quantum Radiophysics Laboratory in the Lebedev Physics Institute, RAS (FIAN), the first-ever successful experiment on the initiation of a thermonuclear reaction by high-power USP irradiation of a lithium deuteride target was implemented in 1968 [3]. The pulse energy amounted to 20 J for the pulse duration 20 ps. This 25 m long facility, which was the world's highest-power facility at that time, delivered no more than one pulse in

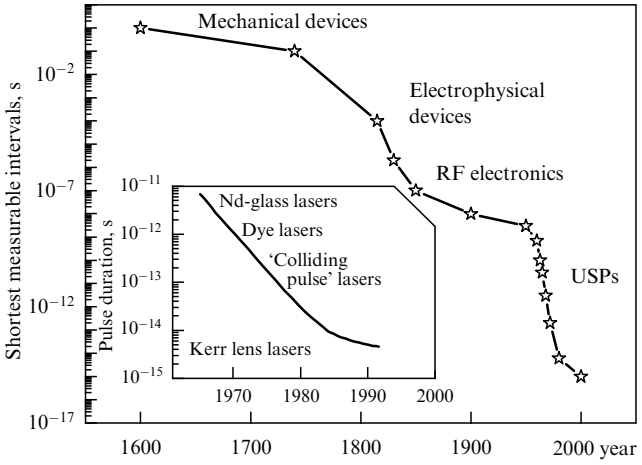

Figure 1. Progress in the measurement of short time intervals during the last four centuries. The inset shows the dynamics of USP duration shortening over a period of 20 years.

15 min, the pulse-to-pulse scatter in the output energy amounting to several hundred percent. The temporal pulse structure was poorly reproducible and the spatial energy distribution in the laser beam was strongly nonuniform due to the multimode radiation nature aggravated by small-scale focusing in the active medium. Nevertheless, also performed at that time were temporal measurements (actually the pioneering measurements of the pump–probe type) to investigate the dynamics of heating and expansion of high-temperature laser-produced plasmas [4] and to observe the emergence and relaxation of refractive index gradients in liquids [5]. Further progress in the USP-assisted investigation of ultrafast processes is associated with the passage to the femtosecond duration range. The subpicosecond structure of USPs was observed even in the first neodymium-glass lasers [6]. The mechanism of femtosecond pulse generation in the radiation self-focusing in the active element [7] was also elucidated at that time. However, subsequent progress in femtosecond technology followed the path of dye lasers. A laser based on self-focusing in an active medium as an instrument of the femtosecond pulse formation was put in operation almost 20 years later [8], and just this kind of solid-state laser (referred to as 'third-generation lasers' [1]) has now gained the widest acceptance.

In 1973, at the Institute of Spectroscopy of the RAS (ISAN), work began on USP applications in scientific research involving picosecond lasers (see Ref. [9] and the references therein). The USSR's first femtosecond USP dye oscillator was put into service at ISAN in 1979 [10]. But it took several additional years to develop the amplifiers and the multichannel recording system required to carry out experiments in ultrafast dynamics with a femtosecond time resolution. Comparing the parameters of the resultant femtosecond laser system with those of the aforementioned USP laser of 1968 shows that apart from shortening the duration (100–300 fs instead of 20 ps), a significant improvement was achieved in the reproducibility of the temporal pulse shape and the output pulse energy (the scatter was within 10%), as was an improvement in uniformity of the beam energy distribution. For the output energy 1 mJ, it was possible to attain at-focus radiation intensities up to 10^{15} W cm^{-2}, i.e., of the same order of magnitude as in thermonuclear investigations [3]. However, the radiation self-focusing in the optical elements of the amplifier was responsible for a severe distortion of the temporal pulse profile and the spatial beam energy distribution. Most significant from the standpoint of shortening the duration of experiments was an increase in the 'rate of fire' by almost three orders of magnitude (the pulse repetition rate was several Hertz). Nevertheless, the preparation and pursuance of an experiment at this facility would normally occupy several months (even when working in three shifts).

Several studies of excitation relaxation dynamics were carried out with a femtosecond time resolution at several objects at ISAN in 1985–1995. Investigations were made of energy and charge transfer in bacterial reaction photosynthesis centers [11] and in bacteriorhodopsin [12], photodesorption and selective chromophore photodetachment in molecules adsorbed on a surface [13], the relaxation of photo-excited charge carriers in semiconductor microcrystallites in a glass matrix [14], in polydiacetylene monocrystals [15], and in fullerene [16] and metallic [17] films; the electron–phonon interaction parameter was measured, and an energy gap was observed in high-temperature superconductors [18]. At this stage, the formulation of almost all problems, as well as the interpretation of experimental data, was done by the staff members of the institute. At the end of the 20th century, due to the problem of material and human resources, the outdated equipment was not upgraded and experiments were staged in foreign laboratories. However, due to financial support from the RAS and other organizations, the most modern femtosecond equipment would gradually appear at ISAN, which was collected into a united spectrometric complex within the Collective-Use Center (CUC) organized early in 2004. As different units of this equipment appeared, experiments reliant on new third-generation lasers were resumed at the institute. The experimental capabilities of the complex continue to expand.

2. Femtosecond laser complex of the 'Optical and Spectral Research' Collective-Use Center of the Institute of Spectroscopy, RAS

The complex is accommodated in a specially fitted dust-free hall with the temperature stabilized to within 1 °C. All equipment is accommodated on vibration-proof optical tables from the Standa company mounted on a common isolated base and is covered with a protective housing, with a low excess pressure maintained inside to keep dust from finding its way into the optical elements (Fig. 2). The complex is comprised of the laser part proper, systems for measuring the pulse parameters, frequency tuning systems, the recording systems for conducting pump–probe type experiments, a photoelectron laser microscope, and auxiliary systems that keep the main units running (power units, cooling units, electronic control units equipped with personal computers, etc.). The main laser components of the complex and their output parameters are diagrammed in Fig. 3. The laser part consists of a 'Tsunami HP' femtosecond pulse oscillator and a 'Spitfire HP' regenerative amplifier made by Spectra Physics. The oscillator is pumped at the wavelength 532 nm by a cw diode-pumped solid-state 'Millenia-V' Nd:YVO_4 laser with the output power 4.5 W. The amplifier is pumped by a pulsed diode-pumped solid-state 'Evolution-X' Nd:YLF laser with the average output power 8 W at the wavelength 527 nm for the pulse repetition rate 1 kHz.

Figure 2. General view of the femtosecond laser complex of the 'Optical and Spectral Research' CUC at ISAN.

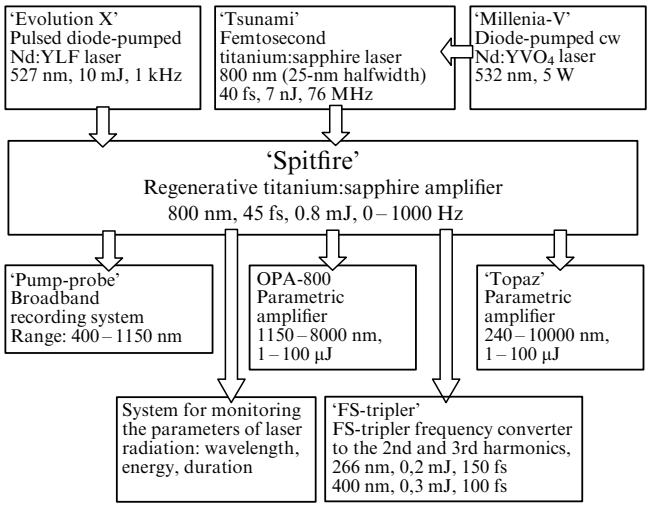

Figure 3. Schematic diagram showing the main laser components of the 'Optical and Spectral Research' CUC at ISAN.

It is pertinent to note that third-generation amplifiers use chirped pulse amplification [1], and the limitations normally imposed by self-focusing in the amplifier stages and its associated temporal and spatial pulse distortions are therefore nonexistent in this case. The energy of 800 nm femtosecond pulses at the amplifier output may amount to 1 mJ for the pulse length 45 fs and the repetition rate 1 kHz. The spectral pulse halfwidth (FWHM) is equal to ~ 20 nm. The energy distribution over the beam section is close to the diffraction-limited Gaussian one, the pulse-to-pulse parameter scatter is within 1%. This parameter is extremely important for stable pulse production in nonlinear frequency conversion and allows obtaining a broad tuning range. The pulse-to-pulse parameter reproducibility is most significant in experiments of the pump–probe type, which involve data averaging over several thousand pulses.

The high beam quality enables the easy production of intensities above 10^{16} W cm^{-2} by focusing the pulse at the 800 nm fundamental wavelength. Three parametric amplifier systems afford frequency tuning. Two of them operate in the near-IR range (from 1150 to 8000 nm), the third is a universal 'Topaz' parametric amplifier operating with a continuous tuning in the spectral range from 240 nm to 10 μm. This parameter combination alone makes this complex unique. We emphasize that the facility's 'rate of fire' is three orders of magnitude higher than that of the previous home-made dye system (six orders of magnitude higher in comparison with the 'rate of fire' of the 1968 facility [2]), apart from quite a substantial broadening of the spectral range. A unique multichannel recording system developed by the Russian 'CDP Systems' company (Troitsk) enables a full realization of these advantages in pump–probe type experiments, which are most often used to study the dynamics of ultrafast processes. The employment of linear diode arrays in lieu of CCDs (charge-coupled devices) for the broadband recording of difference spectra enables operation at the repetition rate 1 kHz (linear CCD arrays can be operated at repetition rates up to several dozen Hertz). This shortens the duration of an experiment by three orders of magnitude in comparison with the time required to carry out the experiment on the previous system.

3. Experiments at the facilities of the Collective-Use Center

Below, we briefly describe the main areas of experiments on the unique spectrometric complex that are underway or planned for the nearest future. These areas can be related to the main objects under investigation.

3.1 Photoelectrons

3.1.1 Laser photoelectron microscope. Schematically, a photoelectron projection microscope is a pointed needle with a curvature radius r_c placed in a vacuum chamber. A special holder firmly secures the needle at the distance $L = 10$ cm from the detector, which consists of a microchannel plate and a phosphorescent screen (Fig. 4a). A potential of 0–4 kV is applied to the sample; when this potential is high enough, efficient field (tunnel) emission of electrons from the tip of the needle occurs. The radial electric field directs the emitted electrons to the detector and forms a magnified tip image on the screen. The magnification is given by $K = L/(br_c)$, where b is a numerical factor equal to 1.5–2. In the investigation of the photoelectron image of the needle tip, the needle potential is lowered to a level whereby the tunnel electron emission from the tip is zero, such that electrons are emitted strictly due to the external photoeffect in the needle material. As in the case of field emission, the electric field around the tip directs the emitted photoelectrons to the detector to form a photoelectron image of the tip with the same magnification. When ultrasharp ($r_c = 20$ nm) nanotips of different materials were irradiated by second-harmonic laser pulses with the wavelength 410 nm, pulse duration ≈ 60 fs, repetition rate ≈ 76 MHz, and pulse energy 0.03–0.3 nJ, their photoelectron images were observed and the resolution about 3 nm was obtained [19]. The measured photocurrent was minimally dependent on the tip potential but was proportional to the squared radiation intensity. No photocurrent was observed under irradiation by the fundamental harmonic pulses of a titanium:sapphire laser (with the wavelength 820 nm and the photon energy 1.56 eV) up to intensity values of the order 10^9 W cm^{-2}. The above experimental observations are unambiguous indications that the photoelectron images of the tips arise from two-photon emission due to the action of femtosecond laser pulses with

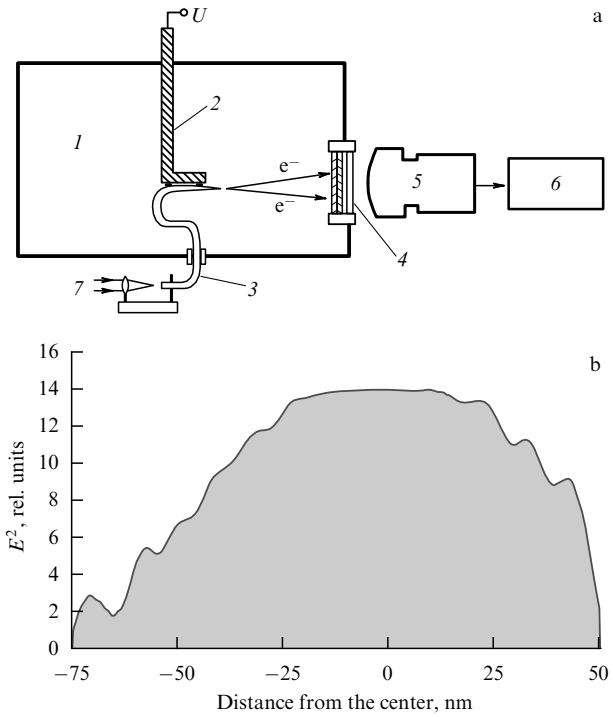

Figure 4. (a) Schematic diagram of the photoelectron microscope in the context of the experiment described in Section 3.1.2: *1* — vacuum chamber, *2* — electrode, *3* — optical fiber, *4* — detector, *5* — TV camera, *6* — special-purpose 'Argus-50' processor, *7* — laser radiation. (b) Distribution of the squared electric field E^2 over the subwave aperture.

the photon energy 3.02 eV. The two-photon photoeffect coefficient was determined for the materials under study. The advantage of this approach in comparison with other 'classic' techniques for measuring the external photoeffect consists in the possibility of obtaining its local values with the spatial resolution as high as 3 nm.

3.1.2 Nonperturbing near-field light measurement. In the experiments in Ref. [20], instead of a nanotip, pointed optical fibers with a metallic coating were used, which had an aperture of the diameter 50–200 nm at the fiber tip transparent to light. These fibers are employed in near-field microscopy. An investigation of the light intensity distribution in a subwave aperture by introducing any sensor into the near-field region is evidently accompanied by a very severe distortion of the initial intensity distribution. For a nonperturbing measurement, the two-photon photoeffect produced by short laser pulses transmitted through the material of the tip was used. In this experiment, femtosecond laser pulses at the wavelength 410 nm were not directed immediately at the tip but were introduced through the other end of the fiber (see Fig. 4). The average power at the waveguide input was limited to a value of 1–3 mW so as not to damage the subwave aperture of the fiber. The light intensity at the fiber output is estimated at $\sim 10^9$ W cm^{-2}. To obtain a 8×10^4-fold magnified image of the tip, a potential of 400–1200 V was applied to the electrode. A quadratic dependence of the photocurrent on the laser radiation power was observed, which was reflective of the two-photon nature of the external photoeffect. The two-photon process efficiency is proportional to the fourth power of the effective electric intensity, E^4. Figure 4b shows the square root of the photocurrent intensity as a function of the distance ρ to the aperture center, i.e., the sought $E^2(\rho)$ distribution.

3.1.3 Visualization of organic nanocomplexes. In the experiment in Ref. [21] in femtosecond laser projection microscopy of organic nanocomplexes, a quartz 100 nm capillary with a nickel layer vacuum-deposited on it was used as a sharp needle. The photoelectron images of two nickel-coated capillaries with deposited-layer thicknesses 25 and 40 nm (Figs 5a and 5b) were observed when the tip was subjected to femtosecond 400 nm radiation. The external static field produced upon applying a negative 300 V potential to the tip decreased the work function, permitting a one-photon electron emission from the metallic surface to be effected by a light photon with $\lambda = 400$ nm. In this case, the recorded photoelectron signal was a linear function of the laser radiation energy. At the next stage, the nickel-coated quartz capillary was wetted with an ethanol solution of Cl53 dye molecules and then dried. When this sample was exposed to femtosecond 400 nm radiation, a quadratic dependence of the photoelectron current on the laser pulse energy was observed and the photoelectron image of the organic nanocomplex on the surface of the nanocomplex was recorded with the spatial resolution about 5 nm (Figs 5c and 5d).

An experiment aimed at obtaining a nanolocalized electron beam with a femtosecond duration intended for use in experiments involving reflection from the evanescent wave produced by a femtosecond laser pulse is presently being conducted.

3.2 Atoms. Projected experiment in atomic physics

Currently, experiments with atoms are in the preparation stage. Investigations of the spatial localization of an atom in the field of periodic femtosecond laser pulses are planned as joint experiments with the ISAN laboratory headed by V I Balykin. The problem is that the potential that localizes an atom in 'stationary' light traps exerts an appreciable perturbing action on the internal and external atomic degrees of freedom. The calculations in Ref. [22] suggest that it is possible to localize a slow atom in the field of colliding femtosecond pulses with an absolute accuracy ranging into the nanometers. In this case, the localization time can be much longer than the atomic spontaneous decay time and 10^7–10^8 times longer than the duration of atomic stay in the laser field.

3.3 Molecules and molecular complexes

3.3.1 Feasibility study of molecular photodissociation by the action of femtosecond IR radiation on overtone vibrations. Femtosecond pulses generated in the near-IR range allow attaining intramolecular selectivity by acting on the vibrational degrees of freedom of molecules in the ground electronic state and by selectively exciting overtones or one of the fundamental vibrations in a shorter time than the characteristic intramolecular vibration redistribution times. This holds some promise that it will be possible to realize photochemical transformations in a molecule that are bond- or bond group-selective. In the first experiments [23] conducted jointly with E A Ryabov's laboratory (ISAN), an investigation was made of the decay of CF_2HCl molecules in the tuning of femtosecond radiation in the region of the overtone transitions of the ν_1 mode (1.3–1.8 μm), as well as at the wavelengths 0.4 and 0.8 μm. The energy of femtosecond pulses at the parametric amplifier output amounted to

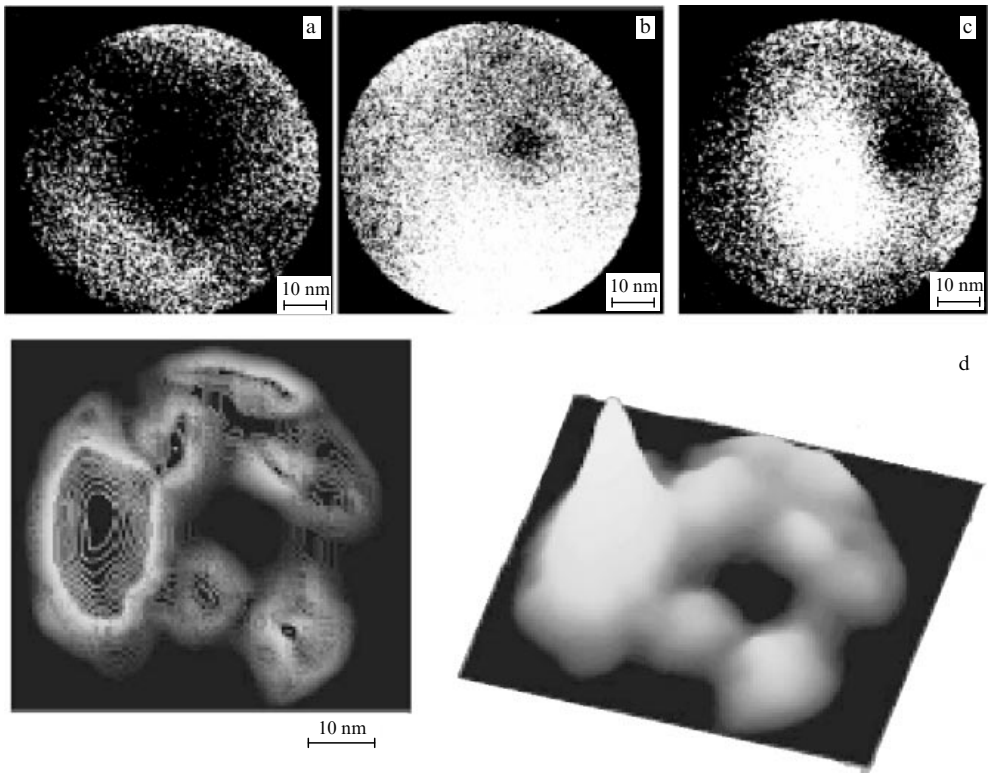

Figure 5. Photoelectron images of a quartz 100 nm capillary coated with a nickel layer of thickness (a) 25 nm and (b) 40 nm, and (c) with an organic nanocomplex on the surface of the point. (d) Images of the same complex for a rotated capillary. The structure height at the right of Fig. 5d corresponds to the magnitude of the photoelectron signal.

50 – 130 μJ at the wavelengths 1.3 – 1.8 μm for the pulse duration $\sim$ 100 fs. The radiation was focused in CF_2HCl at the pressure 1 Torr. The resultant products were analyzed from IR transmission spectra recorded prior to and after the irradiation.

The experiments conducted revealed that the resonances of femtosecond radiation with vibrational overtone transitions at the wavelengths $\lambda_{0\to 2} = 1.69$ and $\lambda_{2\to 4} = 1.82$ μm have little or no effect on the CF_2HCl decay. Only one final dissociation product — CF_3H — was discovered, which substantially differentiates the results of CF_2HCl dissociation under femtosecond pulse irradiation from the results of thermal pyrolysis under the action of infrared or ultraviolet (UV) nanosecond laser pulses. The absence of the effect of femtosecond radiation resonance with vibrational overtone transitions on the decay of CF_2HCl may be due to the low intensity of the overtone transitions and the strong anharmonicity of C – H bond vibrations. This is why the cross section of successive multiphoton transitions is very small and the radiation intensity should be high enough to give rise to the excitation and dissociation of the molecule. For the intensity $\sim 100\ \mathrm{TW\ cm^{-2}}$, the main role in molecular decay is played by field ionization and the contribution of multiphoton excitation becomes insignificant compared with the background of the principal process.

At present, due to the broadening of the IR spectral range of lasers, a start has been made on experiments in selective molecular excitation at the fundamental vibration frequencies of the main bonds.

3.3.2 Investigation of the dynamics and structure of molecular complexes. Among the most powerful instruments suited to this purpose are nondestructive optical techniques, which permit retaining all functional properties of the material under study during investigation. Clearly, the spatial distribution of nanostructure components, as well as the mutual packing of the subunits in the nanostructured material, are critical to the properties of the material as a whole. In turn, information about it can be gained by investigating the relaxation material properties. The nanometer sizes of the subunits suggest that the shortest excitation relaxation times range into the femtoseconds. That is why femtosecond spectroscopy may turn out to be one of the most adequate techniques for investigating and certifying nanostructured materials.

The femtosecond pump – probe technique was used to investigate the dynamics of transmission and reflection difference spectra in two types of objects: in the peripheral pigment – protein complex of the LH2 light-harvesting antenna of the photosynthetic system of the *Trs. sibirica* purple bacteria (in collaboration with the Belozerskii Institute of Physicochemical Biology, Moscow State University) and in heterophase fullerene – metal nanostructures (jointly with FIAN). The pump – probe technique in its various modifications is the main instrument for the investigation of the femtosecond dynamics of fast processes [9]. The information is gathered in the form of a set of difference transmission and/or reflection spectra (the difference of the logarithms of normalized signals with and without excitation) of a sample recorded with a femtosecond exposure at different time instants prior to and after the excitation of the sample by a femtosecond pulse.

Excitation energy transfer between the LH2-complex absorption bands of Trs. sibirica bacteria under excitation by 800-nm femtosecond pulses. The structural basis of the photosynthetic system of purple bacteria is the pigment –

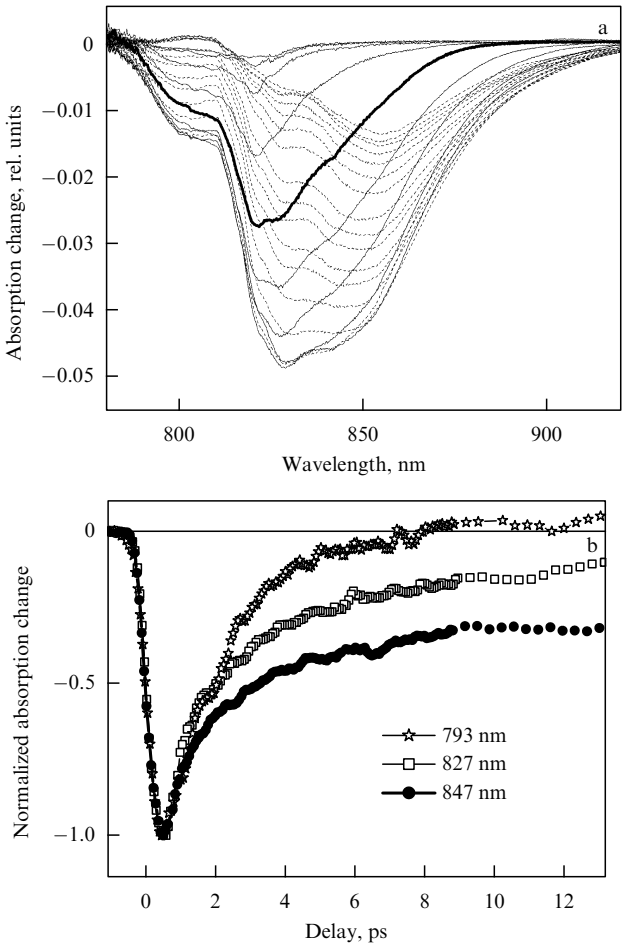

Figure 6. (a) Spectra of the photo-induced optical absorption changes in the LH2 *Trs. sibirica* bacteria complex recorded for different probe pulse delays relative to the excitation pulse. Solid curves show the spectra recorded in the buildup of band bleaching up to the attainment of the strongest effect and the dashed curves show the spectra subsequently recorded during the waning of bleaching. The zero point in time t corresponds to the temporal coincidence of the exciting and probing pulse peaks. The spectrum for $t = 0$ is shown with the bold solid curve. The delay increment is 137 ps. (b) Normalized kinetic curves of the photo-induced optical absorption changes at three wavelengths near the absorption band peaks of the sample.

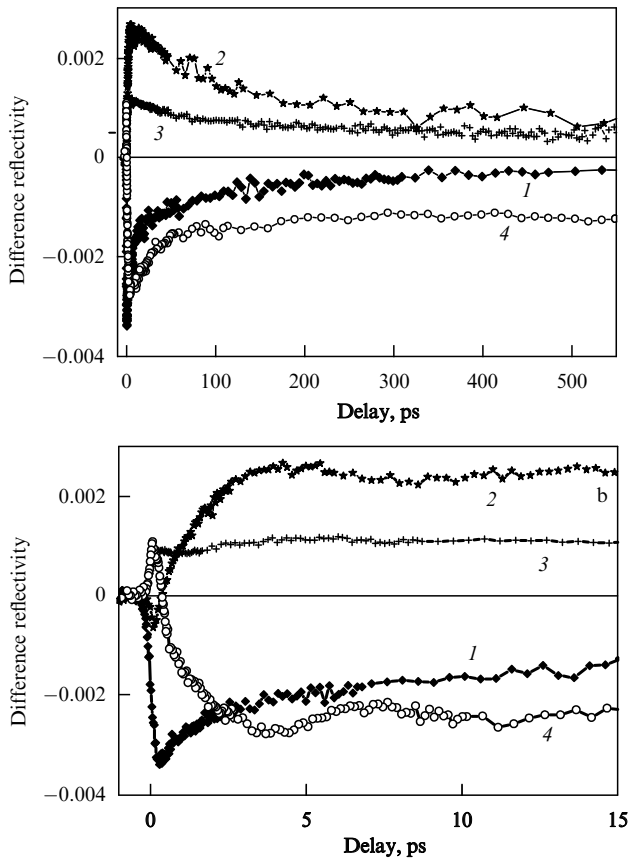

Figure 7. Dynamics of the variation in the difference reflection $\Delta R/R$ (in units of optical density) at the wavelength 1250 nm for C_{60}/Sn films, which were deposited in various regimes, under excitation at the wavelength 400 nm.

protein complexes of the reaction center (RC) and of the light-collecting antenna (the LH1 core complex and the LH2 peripheral complex). The main absorption bands of the LH2 complexes under investigation with peaks at wavelengths about 800, 830, and 850 nm are due to absorption by similar bacteriochlorophyll (BCh) molecules. These BCh molecules make up ring structures with a characteristic dimension of the order of several dozen nanometers, which vary mainly in the number and mutual orientation of the BCh. In our case, these structures are denoted as B800, B830, and B850. The spectra of photo-induced optical absorption changes for the LH2 complex under excitation by a 50 fs long pulse at the wavelength 800 nm are presented in Fig. 6 together with the kinetic curves of the changes in optical absorption for different probe wavelengths in the B800, B830, and B850 bands. Despite a strong band overlap and a fast excitation energy transfer between the components of the complex, the obtained kinetic curves show the dependence of the relaxation character on the structure of the object. The mathematical data processing and simulations of these experiments performed at Moscow State University revealed a significant difference between the electron structure of the BCh molecular ensemble in the complex investigated and the electron structure in the LH2 complexes in other bacteria.

Ultrafast processes in fullerene–metal nanostructures. Heterophase C_{60}/Sn nanostructures were fabricated as 50–150 nm films on thin quartz substrates by vacuum deposition from two different sources for the metal and the fullerene. The diagnostics of the samples thus fabricated, which were performed with the aid of X-ray structural analysis, electron microscopy, and optical and Raman spectra, showed that varying the deposition mode allowed obtaining films consisting of (i) fullerene polymers, (ii) 10 nm tin nanocrystals covered with fullerene anions, (iii) oriented submicron-sized tin crystallites (in fact, purely metallic films), and (iv) amorphous structures containing metal fractals.

The kinetic curves (Fig. 7) obtained for the four above structures (the curves are numbered in accordance with the above structure list) exhibit an extremely high sensitivity of the dynamics of ultrafast photo-induced processes in composite media to the quantitative ratio between the components and their spatial packing. The substantial difference between the relaxation processes observed for samples with various geometries of the nanocomposites arises from the distinctions in charge carrier generation and in charge transfer between the metal and the fullerene and back [25].

3.4 Ultrafast dynamics in some other structures

3.4.1 Measurement of coherent polarization relaxation times T_2 in condensed media by the femtosecond interference spectroscopy technique. The technique can be applied at a low excitation power and is not complicated by the emergence of a parasitic signal for near-zero delay times, which is commonly inherent in the excitation–probing technique. In the experiment in Ref. [26], a 20 fs long pulse from an oscillator was divided with a Michelson interferometer into two identical collinear pulses of similar intensity and polarization, which were directed onto a sample with a controllable delay. Two coherent polarization waves were generated in the sample, which interfered with each other for a time delay comparable with T_2. The resultant interference pattern was recorded by a high-sensitivity detector. The capabilities of this technique were demonstrated by the example of two doped-glass samples with a significantly different broadening of the absorption band (500 and 40 nm). Measurements showed that for the broadband sample, T_2 does not exceed the pulse duration (20 fs), and $T_2 \sim 50$ fs for the narrow-band sample.

3.4.2 Femtosecond dynamics of semiconductor – metal nanostructure cavity modes. The modes of the cavity of a semiconductor film on a metal are a highly sensitive instrument for the detection of ultrafast photo-induced processes at the metal – semiconductor interface [27]. A femtosecond laser pulse gives rise to a photo-induced change in the semiconductor permittivity and hence in the optical thickness of the cavity due to the optical excitation of the semiconductor and/or due to the penetration of electrons into the semiconductor across the Schottky barrier, which results in an ultrafast photovoltaic effect. The change in the metal permittivity under femtosecond irradiation by a laser pulse, which is responsible for an instantaneous change of the cavity boundary conditions, permits observing the generation of photons in a transient resonator (dynamic Casimir effect) and making direct measurements of the dynamics of transient electron tunneling across the barrier (wave-packet tunneling). The experiments are performed by the excitation – probing technique (in collaboration with ISAN laboratories headed by E A Vinogradov and Yu E Lozovik).

Furthermore, the first experiments were carried out to study the effect of femtosecond pulse chirp on the generation of coherent photons in semimetals and narrow-gap semiconductors (jointly with the Institute of Solid State Physics, Chernogolovka).

3.5 Experiments in photo-induced material modification and production of optical elements by femtosecond pulse irradiation

Photo-induced transformations in C_{60} *films* irradiated by femtosecond laser pulses were investigated in Ref. [28]. It was found that no photo-induced oxygen uptake into the film is observed under pulsed irradiation, in contrast to the case of continuous irradiation. This has the effect that the photoproducts produced in these two cases are different.

In the interference of femtosecond pulses in light-sensitive media, it has been possible to produce *achromatic holograms*, in which there is no radiation diffraction related to the periodic hologram structure and its attendant dispersion. A start has been made on experiments aimed at the production of these structures in planar waveguides, which will enable fabrication of two-dimensional holographic structures that are one-dimensional mirrors with a complex curvature; they show promise as achromatic integrated optical elements of a new class (jointly with the Central Design Bureau for Unique Instrumentation, RAS) [29].

Experiments aimed at the *formation of Bragg gratings in optical fibers* with the aid of femtosecond UV pulses (jointly with the Fiber Optics Research Center at the Prokhorov General Physics Institute, RAS) [30] and at *controllable surface modification* [31] are being continued; a start has been made on research into the *self-focusing* of femtosecond pulses in transparent dielectrics (in collaboration with the Physics Department of Moscow State University) and on experiments aimed at effecting the *graphite – diamond phase transition* in a high-pressure chamber under femtosecond pulse irradiation (in collaboration with the Institute of High-Pressure Physics, RAS, and FIAN).

4. Conclusion

Due to a unique combination of the capabilities of the femtosecond laser complex of the 'Optical and Spectral Research' CUC in ISAN, its uses are by no means limited by the avenues of research discussed above. Moreover, the capabilities of the complex are steadily being broadened: in the immediate future, the output pulse energy will increase to 2 mJ and the pulse duration will shorten to 30 fs (these are actually the limiting parameters for the facilities of this class); terahertz radiation has been obtained, which is planned for use in semiconductor research; more sensitive recording systems with cooled radiation detectors capable of operating in the IR range are under development.

Acknowledgements

To conclude, I wish to express my appreciation to S A Aseev, V O Kompanets, P G Kryukov, V B Laptev, Yu A Matveets, B M Mironov, A P Razzhivin, E A Ryabov, S K Sekatskii, A M Smolovich, and N F Starodubtsev for their cooperation, and to V I Balykin, E A Vinogradov, V S Letokhov, and Yu E Lozovik for stimulating discussions.

This work was supported by the Russian Foundation for Basic Research (grant nos 05-02-16857, 05-02-17338, 06-02-16186, and 06-02-16301).

References

1. Kryukov P G *Kvantovaya Elektron.* **31** 95 (2001) [*Quantum Electron.* **31** 95 (2001)]
2. Basov N G et al. *Zh. Eksp. Teor. Fiz.* **57** 1175 (1969)
3. Basov N G et al. *Pis'ma Zh. Eksp. Teor. Fiz.* **8** 26 (1968) [*JETP Lett.* **8** 14 (1968)]; Basov N et al. *IEEE J. Quantum Electron.* **QE-4** 864 (1968)
4. Basov N G et al., in *Kvantovaya Elektronika* Vol. 1 (Ed. N G Basov) (Moscow: Sov. Radio, 1971) p. 4 [*Sov. J. Quantum Electron.* **1** (1) 2 (1971)]
5. Kryukov P G, Matveets Yu A, Chekalin S V *Pis'ma Zh. Eksp. Teor. Fiz.* **15** 147 (1972) [*JETP Lett.* **15** 101 (1972)]
6. Basov N G et al. *Zh. Eksp. Teor. Fiz.* **65** 907 (1973) [*Sov. Phys. JETP* **38** 449 (1974)]
7. Zherikhin A N et al. *Kvantovaya Elektron.* **1** 956 (1974) [*Sov. J. Quantum Electron.* **4** 525 (1974)]
8. Spence D E, Kean P N, Sibbett W *Opt. Lett.* **16** 42 (1991)
9. Letokhov V S et al. *Lazernaya Pikosekundnaya Spektroskopiya i Fotokhimiya Biomolekul* (Picosecond Laser Spectroscopy and Photochemistry of Biomolecules) (Ed. V S Letokhov) (Moscow: Nauka, 1987); Zherikhin A N, Author's Abstract of Thesis for Candidates Degree (Troitsk: Institute of Spectroscopy, USSR Academy of Sciences, 1981); Sharkov A V, Author's Abstract of

Thesis for Candidates Degree (Troitsk: Institute of Spectroscopy, USSR Academy of Sciences, 1981)
10. Matveets Yu A, Semchishen V A *Kvantovaya Elektron*. **6** 848 (1979) [*Sov. J. Quantum Electron*. **9** 503 (1979)]
11. Matveets Yu A, Chekalin S V, Yartsev A P *Pis'ma Zh. Eksp. Teor. Fiz*. **43** 546 (1986) [*JETP Lett*. **43** 707 (1986)]; *Dokl. Akad. Nauk SSSR* **292** 724 (1987); Chekalin S V et al. *FEBS Lett*. **216** 245 (1987); Chekalin S V, Matveetz Yu A, Yartsev A P *Rev. Phys. Appl*. **22** 1761 (1987); Matveets Yu A et al. *Dokl. Akad. Nauk SSSR* **294** 1480 (1987); Matveets Yu A, Chekalin S V, Yartsev A P *Izv. Akad. Nauk SSSR Ser. Fiz*. **53** 1462 (1989)
12. Matveetz Yu A, Chekalin S V, Sharkov A V *J. Opt. Soc. Am. B* **2** 634 (1985); Sharkov A V et al. *Photochem. Photobiol*. **38** 109 (1983); Sharkov A V et al. *Biochim. Biophys. Acta* (*BBA*): *Bioenerg*. **808** 94 (1985); Sharkov A V et al. *Dokl. Akad. Nauk SSSR* **281** 466 (1985)
13. Chekalin S V et al. *J. Phys. Chem*. **92** 6855 (1988); Kozlov A A et al. *Pis'ma Zh. Eksp. Teor. Fiz*. **47** 294 (1988) [*JETP Lett*. **47** 353 (1988)]
14. Lozovik Yu E et al. *Pis'ma Zh. Eksp. Teor. Fiz*. **52** 851 (1990) [*JETP Lett*. **52** 221 (1990)]; Besel' I V et al. *Pis'ma Zh. Eksp. Teor. Fiz*. **59** 376 (1994) [*JETP Lett*. **59** 403 (1994)]
15. Afanas'eva N I et al. *Opt. Spektrosk*. **82** 808 (1997) [*Opt. Spectrosc*. **82** 750 (1997)]
16. Bezel I V et al. *Chem. Phys. Lett*. **218** 475 (1994)
17. Golovlev V V et al. *Pis'ma Zh. Eksp. Teor. Fiz*. **55** 441 (1992) [*JETP Lett*. **55** 450 (1992)]
18. Chekalin S V et al. *Phys. Rev. Lett*. **67** 3860 (1991); Gershenzon M E et al. *Pis'ma Zh. Eksp. Teor. Fiz*. **52** 1189 (1990) [*JETP Lett*. **52** 602 (1990)]; Dobryakov A L et al. *Opt. Spektrosk*. **76** 975 (1994) [*Opt. Spectrosc*. **76** 871 (1994)]
19. Sekatskii S K et al. *J. Phys. Chem. A* **102** 4148 (1998); Sekatskii S K et al. *Zh. Eksp. Teor. Fiz*. **115** 1680 (1999) [*JETP* **88** 921 (1999)]; Sekatskii S K et al. *Nonlinear Opt*. **23** 157 (2000)
20. Sekatskii S K et al. *Appl. Phys. Lett*. **83** 4900 (2003)
21. Aseev S A et al. *Pis'ma Zh. Eksp. Teor. Fiz*. **80** 645 (2004) [*JETP Lett*. **80** 568 (2004)]; Mironov B N et al. *Zh. Eksp. Teor. Fiz*. **128** 732 (2005) [*JETP* **101** 628 (2005)]
22. Balykin V I *Pis'ma Zh. Eksp. Teor. Fiz*. **81** 268 (2005) [*JETP Lett*. **81** 209 (2005)]
23. Apatin V M et al. *Pis'ma Zh. Eksp. Teor. Fiz*. **80** 104 (2004) [*JETP Lett*. **80** 95 (2004)]; Apatin V M et al. *Chem. Phys. Lett*. **414** 76 (2005)
24. Razjivin A P et al. *Biologicheskie Membrany* **2** 55, 83 (2005); *Kvantovaya Elektron*. **35** 107 (2005) [*Quantum Electron*. **35** 107 (2005)]
25. Chekalin S, Kompanets V, Starodubtsev N *Proc. SPIE* **6181** 282 (2006)
26. Kompanets V O, Matveets Yu A, Chekalin S V *Kvantovaya Elektron*. **31** 393 (2001) [*Quantum Electron*. **31** 393 (2001)]
27. Vinogradov E A *Usp. Fiz. Nauk* **172** 1371 (2002) [*Phys. Usp*. **45** 1213 (2002)]; *Laser Phys*. **15** 954 (2005)
28. Kompanets V O et al. *Pis'ma Zh. Eksp. Teor. Fiz*. **68** 320 (1998) [*JETP Lett*. **68** 344 (1998)]
29. Dement'ev D A et al. *Pis'ma Zh. Eksp. Teor. Fiz*. **65** 388 (1997) [*JETP Lett*. **65** 402 (1997)]; *Opt. Commun*. **150** 38 (1998); Aseyev S A et al. *Proc. SPIE* **6181** 274 (2006)
30. Zagorulko K et al. *Opt. Express* **12** 5996 (2004)
31. Lozovik Yu E et al. *Laser Phys*. **9** 564 (1999)

PACS numbers: **03.67.–a**, **71.35.–y**, **76.30.–v**
DOI: 10.1070/PU2006v049n06ABEH006045

Time-resolved EPR spectroscopy of nonequilibrium spin systems produced during spin-dependent photophysical and photochemical processes in condensed media

K M Salikhov

1. Introduction

The course of spin-dependent elementary acts may result in the formation of nonequilibrium polarization of electron spins exceeding the equilibrium spin polarization by several orders of magnitude. The physical nature of the nonequilibrium polarization formation is as follows. In elementary photophysical and photochemical events, it is not infrequent that the Hamiltonian of spin systems changes rapidly on a time scale of spin evolution times, and therefore the spins do not follow the variations in the spin Hamiltonian parameters adiabatically. For instance, in the rupture of a chemical bond, two free radicals form that inherit the spin state of the molecule. For these nonadiabatic processes, the disintegration of the molecule is, with respect to the spins of valence electrons, an abrupt switch of the spin Hamiltonian: a large value of the exchange integral in the molecule rapidly gives way to a relatively small value for two radicals at the distance equal to the sum of their Van der Waals radii; the *g*-factor of unpaired electrons changes simultaneously. The molecular spin Hamiltonian does not commute with the spin Hamiltonian of the two resultant radicals and therefore the electron spins of the radicals at the instant of radical pair production find themselves in a transient coherent state [1]. A similar situation occurs in the photo-induced electron transfer.

The above scheme of the transient spin state formation may formally be represented as follows. We let H_1 and ψ_n denote the spin Hamiltonian and eigenstates of the system *prior to* a phototransformation and H_2 and φ_p denote the spin Hamiltonian and eigenstates of the system *after* the phototransformation.. We assume that the phototransformation occurs in an excited state ψ_2 and the event proceeds nonadiabatically. In this situation, the phototransformation products (for instance, a pair of radicals resulting from molecular photodecay or an electron–hole pair produced in the phototransfer of an electron) are produced in the initial state with the wave function ψ_2, which is not an eigenfunction for the products because the spin Hamiltonians H_1 and H_2 do not commute, as a rule. This initial state can be represented as a linear superposition of the eigenstates of the products: $\varphi(0) = \psi_2 = \sum c_p \varphi_p$. The subsequent evolution of the electron spins is described by the wave function

$$\varphi(t) = \sum c_p \exp\left(-\frac{\mathrm{i}E_p t}{\hbar}\right) \varphi_p \,, \qquad (1)$$

where E_p are the energy levels upon phototransformation.

Therefore, by inducing nonadiabatic transformations by a light pulse, it is possible to prepare ensembles of electron spin systems in transient coherent states.

In free-radical or electron–hole pairs, the evolution of wave packet (1) quite frequently proceeds on the nanosecond time scale [1]. Modern techniques of electron paramagnetic resonance (EPR) also permit observing the evolution of transient electron spin states with a nanosecond resolution. Directly observable in EPR experiments is the dipole spin polarization. In the phototransformation of diamagnetic molecules in the initial state ψ_2, the electron spins are not polarized, and therefore the EPR signal cannot be observed immediately in the products of nonadiabatic reactions. However, the spin dynamics are responsible for the formation of the EPR-observable polarization of electron spins.

We note that elementary photo-induced nonadiabatic reactions allow preparing ensembles of electron spins in the initial states unattainable when starting from the thermodynamic equilibrium. That is why the results of investigations of paramagnets at thermal equilibrium are not directly